

Final Report

# Novel Hydrogen Sulfide Sensors for Portable Monitors

Contract 1 R43 OH07471-01  
SBIR Phase I

SUBMITTED BY



**NANOMATERIALS**  
RESEARCH

2021 Miller Drive  
Longmont, CO 80501

Principal Investigator: M.W. Hooker

Co-investigators: E.J. Benstock, D.J. Deininger, S.A. Hooker, C.J. Kostelecky, S.S. Williams, and K. Womer

Tel: (720) 494-8401 • Fax: (720) 494-8402

7/16/02

INFORMATION CONTAINED HEREIN IS PROPRIETARY FOR 4 YEARS IN ACCORDANCE  
WITH FAR 52.227-20

## TABLE OF CONTENTS

1. List of Abbreviations.....	2
2. List of Figures.....	3
3. List of Tables.....	4
4. Abstract.....	5
5. Significant Findings.....	5
6. Usefulness of Findings.....	6
7. Scientific Report.....	7
7.1 Significance of the Problem.....	7
7.2 Phase I Objectives.....	10
7.3 Phase I Results.....	11
7.3.1 Preparation of Sensing Elements.....	11
7.3.2 Characterization of Sensing Elements.....	15
7.4 Commercialization Potential.....	23
7.5 Phase I Conclusions and Outlook for Phase II.....	27
8. Publications.....	28
9. References.....	29

### 1. LIST OF ABBREVIATIONS

Gold (Au)  
Hydrogen sulfide (H<sub>2</sub>S)  
Indium tin oxide (ITO)  
Micrometers (μm)  
Nanomaterials Research, LLC (NRLLC)  
Nanometers (nm)  
Ohms (Ω)  
Parts per million (ppm)  
Platinum (Pt)  
Resistance in air (R<sub>a</sub>)  
Resistance in gas (R<sub>g</sub>)  
Scanning electron microscope (SEM)  
Tungsten oxide (WO<sub>3</sub>)  
Volts (V)  
Watts (W)

## 2. LIST OF FIGURES

Figure 1: Schematic of a multilayer ceramic component and a SEM micrograph showing a multilayer capacitor produced at NRLLC. The bright regions represent the individual electrode layers within the device.....	9
Figure 2: Control charts showing the deviation of the resistance values of multilayer thermistors (left) and screen-printed composite sensor materials (right).....	9
Figure 3: Theoretical resistance of a multilayer sensor as a function of layer thickness and the number of metal oxide layers. In this example, a 1206 (0.120" x 0.060") chip size and a resistivity of 21,000 $\Omega$ -cm were assumed. ....	10
Figure 4: Flow diagram showing the multilayer sensor fabrication process.....	12
Figure 5: Thermal profile used to remove the organic materials from the tape cast parts. ....	14
Figure 6: Typical example of the firing profile used to sinter the WO <sub>3</sub> /ITO multilayers. ....	14
Figure 7: SEM micrographs showing the decreasing porosity obtained as the sintering temperature is increased. The above images were obtained from specimens fired at 975°C (upper left), 1025°C (upper middle), 1050°C (upper right), 1075°C (lower left), 1100°C (lower center), and 1125°C (lower right).....	15
Figure 8: Photographs showing the hazardous gas test system in a fume hood (left) and a close-up image of the test apparatus (right). ....	16
Figure 9: Typical response of 85/15 WO <sub>3</sub> /ITO multilayer sensors to 20 ppm H <sub>2</sub> S at 200°C (lot number AB-313-01b). ....	18
Figure 10: Response to 20 ppm H <sub>2</sub> S for a typical WO <sub>3</sub> sensor operated at 300°C. ....	18
Figure 11: Typical response to repeated exposures to 20 ppm H <sub>2</sub> S.....	19
Figure 12: Effect of different H <sub>2</sub> S concentrations on WO <sub>3</sub> sensor response when operated at 300°C. ....	19
Figure 13: Optical microscope image of a WO <sub>3</sub> multilayer with one active internal layer. ....	20
Figure 14: Response of a typical WO <sub>3</sub> sensor produced with only one active layer. Sensor was exposed to 20 ppm H <sub>2</sub> S in dry air at both 200 and 300°C. ....	20
Figure 15: Responses to 20 ppm H <sub>2</sub> S for components prepared from different powders. ....	21
Figure 16: Effect of processing temperature on gas response.....	22

3. LIST OF TABLES

Table 1: Effects of H<sub>2</sub>S on humans following exposure to specific concentrations [,]..... 7

Table 2. Summary of multilayer sensor designs produced during Phase I..... 13

Table 3. Porosity of WO<sub>3</sub> multilayers fired at temperatures from 975 to 1125°C..... 15

Table 4. Typical response of prototype multilayer sensors (lot number H2S-AB-313-01) to 20 ppm H<sub>2</sub>S at 25, 50, 100, and 200°C..... 18

Table 5. Effect of operating temperature on response and recovery of a typical batch of WO<sub>3</sub> multilayer sensors containing one active internal layer. Each data point represents the average of 5 sensors tested simultaneously..... 20

Table 6. Powder characteristics for the different WO<sub>3</sub> materials. All materials were prepared from the same lot of powder received from the vendor..... 21

#### 4. ABSTRACT

During this SBIR Phase I project, Nanomaterials Research (NRLLC) successfully demonstrated a new type of sensor device for detecting hydrogen sulfide (H<sub>2</sub>S). This gas is extremely toxic at low concentrations, and workplace exposure is common in a number of industries. Improved sensors and gas detection instruments are sorely needed to ensure protection of these exposed workers and to reduce H<sub>2</sub>S emissions into the atmosphere, thereby affecting public health.

NRLLC's new sensor device combines recent advances in both semiconductor materials and alternative sensor fabrication approaches. These novel components were produced using processes and architectures that are similar to those used in the manufacture of multilayer ceramic capacitors. The sensors had a footprint of only 0.45 cm x 0.30 cm and exhibited the requisite mechanical strength needed for handling and integration into traditional electronic packages.

The sensors responded well to H<sub>2</sub>S at concentrations ranging from 5 to 50 ppm. These levels are commensurate with the monitoring requirements for workplace exposures, in which the personal exposure limit, or PEL, is 10 ppm and the short-term exposure limit, or STEL, is 15 ppm. The sensors exhibited a large decrease in resistance when the toxic gas was present, which is characteristic of n-type semiconductor behavior. This response was found to be linear with concentration and repeatable during multiple exposures. Response times ( $t_{50}$ ) were on the order of 20 seconds.

Several variables were investigated to determine their effect on the sensor response and recovery. These included the composition of the sensor material, the operating temperature of the device, the particle size of the raw materials, the design of the multilayer structure, and the degree of porosity retained in the final device. While a more extensive study is required, the Phase I results suggest that the processing and operation of the devices can be optimized by controlling such variables, thereby ensuring reliable gas detection. In addition, such devices can be designed to meet specific instrumentation requirements.

The small size and tailorability of NRLLC's sensor devices are important features for implementation of the sensors in gas detection instruments. NRLLC envisions a number of different application scenarios for these sensors including their use in stationary industrial monitoring systems, hand-held detection equipment, and revolutionary new personal monitors based on smart card technology. During the Phase II program, NRLLC plans to explore all three application areas, while building on the Phase I results to optimize sensor performance.

This report summarizes the results of our Phase I SBIR project and discusses the potential market opportunities for these unique devices. Details regarding the investigations performed and the primary results obtained are included. In addition, specifics regarding three primary markets for the technology are provided. Additional market information will be included in the Phase II proposal.

#### 5. SIGNIFICANT FINDINGS

This SBIR project demonstrated a number of significant findings related to Nanomaterials Research's new solid-state H<sub>2</sub>S sensor.

1. The sensors are sufficiently robust after fabrication. This feature is important as the sensors must be handled, packaged, and integrated into instrumentation for final use.

2. The sensors can reliably detect H<sub>2</sub>S vapors from 5 to 50 ppm. This range is important for a number of industrial monitoring applications.
3. The sensor response is linear with concentration. This finding demonstrates that the sensors can be used for quantitative measurements.
4. The sensor response is repeatable during multiple exposures. This finding indicates that the sensors can be used for continuous monitoring or for cumulative exposure testing.
5. The response time is below one minute. This finding indicates that the sensors can be used for real-time monitoring applications.
6. Sensor response can be enhanced by controlling both the sensor composition and the particle size of the raw materials. This finding confirms that both of these variables are important and must be optimized and controlled in the final product.
7. Sensor recovery can be enhanced by controlling the operating temperature of the sensors. This result confirms that the resistance of the sensor in gas varies with temperature in a complex fashion, which can then be used to optimize sensor response during operation. In addition, this finding indicates that pulse heating operational modes may be employed to promote specific reactions while reducing the total power consumption for measurement.
8. The baseline resistance of the sensors can be tailored by adjusting the multilayer configuration. As anticipated, devices with only one large active layer were found to exhibit higher resistances in air than devices with eight internal active layers. This result confirms that the multilayer design can be used to tailor the electrical properties of the device as needed by instrumentation. This degree of control is not feasible with conventional sensor fabrication processes.
9. The degree of porosity in the sensor device can be tailored by controlling the thermal profile and can be used to optimize the magnitude of the sensor response. This result confirms that microstructure plays an essential role in device performance. However, a more extensive study is required as changes in thermal treatment can also affect sintered grain size, compositional phase, and oxidation state. If a more comprehensive understanding of the effects of these variables can be developed during Phase II, the ability to design and fabricate optimized sensors will be vastly improved, benefiting the entire field of resistive gas sensors.

## 6. USEFULNESS OF FINDINGS

The Phase I findings are significant in that they confirm that Nanomaterials Research's patented multilayer fabrication process can be successfully transitioned into a working sensor device of substantial interest to the industrial hygiene community. This process offers advantages in tailorability, reproducibility, and cost-effectiveness that are unparalleled in conventional sensor manufacture. In addition, chip-style sensor components open the door to revolutionary approaches to personal exposure monitoring, including the potential for direct integration of the sensors with smart card technology. The resulting gas detection system can then be fully contained on a personal exposure badge, providing quantitative, real-time exposure information and alarm capabilities. Such devices can greatly improve individual worker safety, particularly when compared with conventional colorimetric H<sub>2</sub>S detectors.

## 7. SCIENTIFIC REPORT

### 7.1 SIGNIFICANCE OF THE PROBLEM

Hydrogen sulfide is a colorless gas that has a foul odor (a rotten egg smell) and is slightly heavier than air. It is flammable between approximately 5 and 40% in air and is acutely toxic, even at low concentrations. Human exposure to even small amounts of hydrogen sulfide can cause headaches, nausea, and eye irritation. Higher concentrations can cause respiratory system paralysis, resulting in fainting and possible death. Table I summarizes the effects of H<sub>2</sub>S exposure on human health.

**Table I: Effects of H<sub>2</sub>S on humans following exposure to specific concentrations [1,2].**

H <sub>2</sub> S Level	Resulting Effects and Regulated Exposure Limits
1-5 ppm	Detectable by smell
10 ppm	Beginning eye irritation
100 ppm	Coughing, eye irritation, loss of smell after only a few minutes
300-500 ppm	Conjunctivitis and respiratory tract irritation, loss of consciousness (~30 min), possible death, artificial resuscitation necessary
700-1000 ppm	Immediate respiratory arrest and loss of consciousness, permanent brain damage, death

Hydrogen sulfide is encountered in a wide range of occupations, and a number of relevant standards have been established for occupational exposure. For example, the OSHA Permissible Exposure Limit (PEL) for H<sub>2</sub>S is 10 ppm (8-hour time-weighted average). The Short Term Exposure Limit (STEL) is 15 ppm (15-minute time-weighted average). Exposures of 300 ppm or greater are considered immediately dangerous to life and health (IDLH) [3].

The above regulatory values clearly indicate the importance of early detection and monitoring of H<sub>2</sub>S at concentrations of 100 ppm or lower in order to prevent its toxic influence. Operations that potentially contribute to H<sub>2</sub>S emissions now routinely require certification for compliance. The analysis techniques and equipment used to accomplish certification are often based on batch sampling followed by laboratory analysis [4], and thus are time consuming. Attempts to adapt these methods to real-time process control and continuous compliance monitoring have met with limited success.

Technologies normally used for gas monitoring, such as electrochemical cells and SnO<sub>2</sub>-type solid-state sensors, suffer from significant limitations with respect to detection of hydrogen sulfide. Electrochemical sensors are relatively expensive (\$100-300) and typically last only 12-24 months. Furthermore, this life span is often significantly reduced when the sensors are exposed to very high concentrations of H<sub>2</sub>S, particularly in combination with high humidity levels [5]. Such environments are routinely encountered in confined spaces such as manholes, drilling wells, and underground storage vessels, where monitoring of H<sub>2</sub>S is particularly important for worker safety.

Alternatively, conventional solid-state sensors, manufactured mainly by Figaro and Capteur, are relatively inexpensive (less than \$50) and long lasting. However, these sensors are known to suffer from a lack of selectivity and stability, particularly in the presence of sulfur-containing chemical species. A new sensor that is low cost, low power, long lasting, accurate and selective is of great importance for real-time protection of workers from H<sub>2</sub>S exposure.

## Sensor Background

Despite the known problems frequently associated with SnO<sub>2</sub> sensors, such devices are often used due to their low cost and the simplicity of their associated circuitry. These sensors change electrical resistance upon interaction with gaseous molecules at elevated temperatures (typically 250-600°C). For example, a space-charge region is created on the surface of the sensor material due to oxygen adsorption. Thus, negatively charged oxygen ions, O<sub>2</sub><sup>-</sup>, are created on the surface by removing an electron from the conduction band. A similar reaction occurs when reducing gases interact with the surfaces, resulting in adsorbed positive ions on the surface and donation of electrons to the conduction band. In both cases, the result is a narrowing or widening of the band gap. For example, narrowing of the band gap in n-type semiconductors creates an accumulation of negative charges and an increase in conductivity, while widening results in depletion of negative charges and a decrease in conductivity.

Williams recently reviewed gas-sensing applications of semiconducting oxides [6]. Several research groups have studied various metal oxides as H<sub>2</sub>S sensors including SnO<sub>2</sub> [7,8], gold-doped WO<sub>3</sub> [9], and a solid solution of CuO and SnO<sub>2</sub> [10,11,12]. However, all of these sensors have suffered from significant limitations, such as high operating temperature, lack of selectivity, or poor sensitivity at low H<sub>2</sub>S concentrations.

Metal oxide H<sub>2</sub>S sensors based on SnO<sub>2</sub> are currently commercially available and are marketed by a number of companies including Figaro (Japan), Capteur (UK), General Monitors (US), and Pem-Tech (US). They find primary application in the chemical and petrochemical industries. However, as previously discussed, these sensors, which operate at about 350°C, are relatively non-selective. Consequently, other gas species (e.g., CH<sub>4</sub>, H<sub>2</sub>, and CO) can be readily detected along with H<sub>2</sub>S, complicating the output signal. Furthermore, changes in the relative humidity present can significantly impact response, particularly in the case of the Figaro TGS825 H<sub>2</sub>S sensor. Due to the serious risks associated with H<sub>2</sub>S exposure, marked improvements in sensing technology, including species discrimination, are sorely needed.

## Multilayer Sensor Morphology ♦

Solid-state sensors are currently fabricated as either beads (Taguchi-type) or thick film ("planar") devices. Both manufacturing approaches involve a considerable amount of manual labor during fabrication, resulting in limits to reproducibility. Furthermore, these methods are not particularly amenable to automation. Consequently, cost reductions and reproducibility improvements are difficult. In this work, we proposed to use an alternative, patented fabrication process, currently under development at NRLLC, which we anticipate will overcome these disadvantages and ensure high reproducibility at low cost.

This new approach involves the production of chip-style sensor devices with a layered design and a series of internal electrodes. Such components are produced by casting thin ceramic sheets (in this case, using specific oxide materials that are sensitive to H<sub>2</sub>S) with a doctor blade process [13,14]. Electrodes are then deposited on certain sheets using thick-film processes, and the electrode and ceramic layers are interleaved to form the desired "multilayer" assembly. Figure 1 shows an example of this architecture, as well as the cross-section from a multilayer electronic component produced at NRLLC. This example has thirty ceramic layers, and the thickness of each is 17 μm. The thickness of each internal electrode layer is 2 μm.

Multilayer processes are currently used to produce a variety of low-cost electronic components including capacitors, varistors, and thermistors. These parts range from a few cents per part to a few dollars depending on their complexity, footprint, and production volume. Using this approach to manufacture gas sensors offers several advantages compared to bead and thick-film techniques. These include:

- Higher part-to-part reproducibility
- Tailorable baseline resistance values
- Lower manufacturing cost (possibly less than \$3 each including packaging)

As shown in Figure 2, the resistances of multilayer devices are typically much more reproducible than thick-film sensors. In this example, the resistance of multilayer thermistors was found to vary by less than 7.5% whereas the resistance of screen-printed sensors varied greatly (similar to that reported by other gas sensor companies). This reproducibility is directly attributable to the degree of thickness control that is maintained during the process (layer thickness typically varies by less than  $0.25 \mu\text{m}$ ) and the degree of automation achieved.

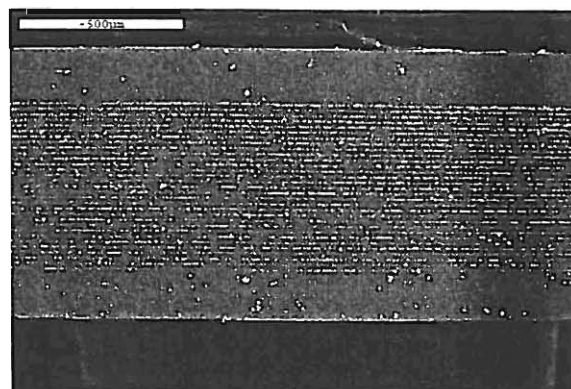
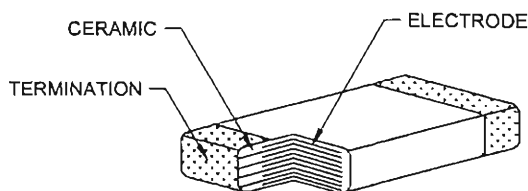


Figure 1: Schematic of a multilayer ceramic component and an SEM micrograph showing a multilayer capacitor produced at NRLLC. The bright regions represent the individual electrode layers within the device.

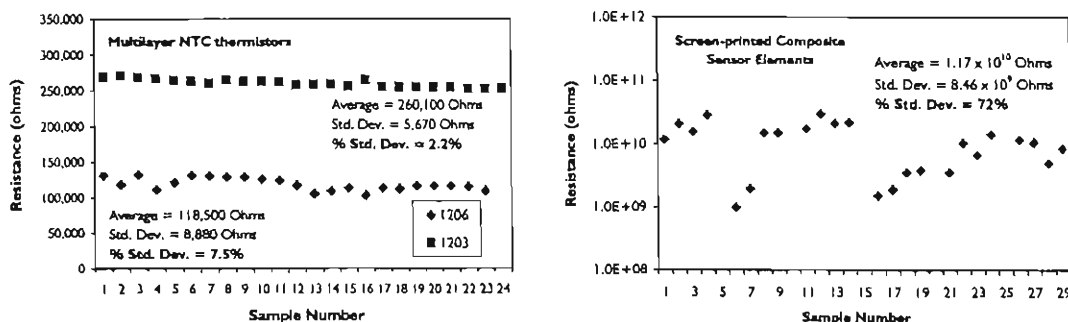


Figure 2: Control charts showing the deviation of the resistance values of multilayer thermistors (left) and screen-printed composite sensor materials (right).

In addition to high reproducibility, this technique also enables the production of devices with a specific resistance value. The resistance of a multilayer device is calculated using the relation:

$$R = \frac{\rho t}{nA}$$

where  $R$  is the resistance of the multilayer element,  $\rho$  is the resistivity of the sensor material,  $t$  is the layer thickness,  $n$  is the number of layers, and  $A$  represents the area under the electrode.

The flexibility provided by this new approach is shown graphically in Figure 3. In this example, the resistance of chip-style multilayer sensors with internal layers of 10, 25, 50, 100, and 200  $\mu\text{m}$  is shown versus the number of layers in the design. As the resistivity of a material is constant, the target resistance of the multilayer device can be readily designed to meet customer specifications without changing the overall footprint of the component. In this example, resistance values ranging from 10 to 10,000  $\Omega$  are illustrated.

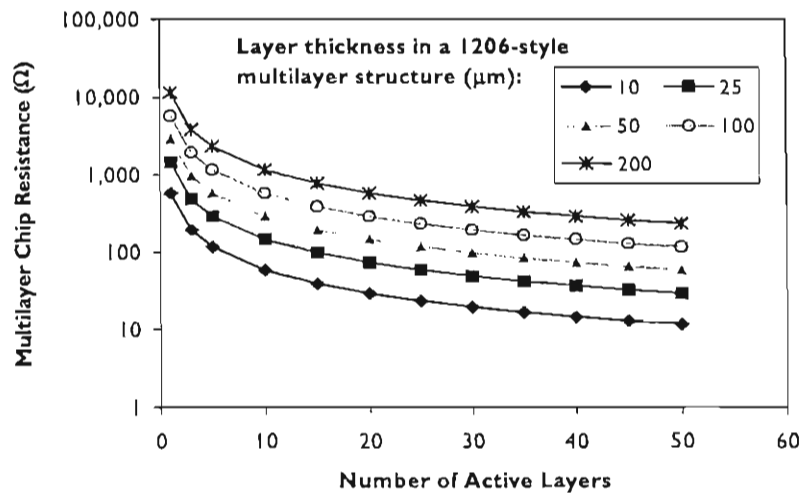


Figure 3. Theoretical resistance of a multilayer sensor as a function of layer thickness and the number of metal oxide layers. In this example, a 1206 (0.120" x 0.060") chip size and a resistivity of 21,000  $\Omega\text{-cm}$  were assumed.

The advantages associated with precise tailoring of the baseline resistance of the sensor material become increasingly important when one begins to consider the steps involved in the development of affordable electronics for receiving and processing sensor outputs. Certain sensor materials exhibit very high electrical resistance values, requiring complicated electronics that can precisely monitor resistance values well into the  $\text{M}\Omega$  range. Meanwhile, other sensor materials have very high conductivity, making it difficult to discriminate small changes in resistance as the sensor is exposed to gas (for n-type semiconductors where resistance decreases in the presence of gas). To date, only limited techniques have been available to tailor the resistance of the sensor, the majority of which involve the addition of secondary phases to the base sensor composition. These secondary materials must be thoroughly evaluated to ensure that no adverse affects on sensor response occur due to their presence. A method of precisely tailoring resistance without the addition of additive materials is of great interest to sensor designers.

## 7.2 PHASE I OBJECTIVES

The primary objective of this SBIR research program is to develop a new type of  $\text{H}_2\text{S}$  sensor based on NRLLC's patented multilayer architecture and nano-scale sensing materials. The resulting sensor will be cost-effective, stable, highly sensitive to low concentrations of  $\text{H}_2\text{S}$ , and highly selective in the presence of other gases. To demonstrate concept feasibility during Phase I, preliminary

prototype devices were fabricated, and their response to H<sub>2</sub>S under a range of operational conditions was evaluated. Specifically, the Phase I work plan listed the following major objectives:

1. **Fabrication of preliminary prototype H<sub>2</sub>S sensor devices using multilayer processing.** Tasks required for this portion of the work included preparation of the raw materials, development of suitable casting “slips”, identification of appropriate internal electrode inks, and preliminary optimization of the processing parameters. The development of devices with sufficient mechanical integrity as to allow for mounting and testing for sensor response was the primary objective.
2. **Characterization of H<sub>2</sub>S response.** Sensor evaluation involved applying gaseous test mixtures to the different devices under a variety of controlled laboratory conditions. The company’s custom-designed and automated hazardous gas test platform was used for these studies. This system allowed for variations in the sensor operating temperature, the concentration and flow rate of the gas applied, and the degree of humidity present in the gas stream. In particular, H<sub>2</sub>S levels from 5 to 50 ppm were studied to meet the existing regulatory requirements for workplace alarms (e.g., PEL of 10 ppm and STEL of 15 ppm).
3. **Relating sensor microstructure to gas response.** In addition to the primary goal of fabricating sensor devices with sufficient mechanical integrity, the effect of sensor microstructure, and in particular device porosity, was also investigated. Conventional thick-film sensors are typically prepared with very high porosity to enable gas flow through the sensor material. However, in the multilayer architecture, the devices must be self-supporting, and such devices are, therefore, typically much denser. To determine the effect of porosity, different microstructures were prepared by adjusting the heat treatment process, and the sensors’ response to 20 ppm H<sub>2</sub>S in air was evaluated.
4. **Further definition of application requirements.** A number of industries are required to monitor H<sub>2</sub>S vapors to ensure worker safety. Examples include agricultural operations; chemical processing and manufacturing plants; road construction sites; natural gas production, processing and transport facilities; petroleum refineries; and waste treatment operations. To commercialize Nanomaterials Research’s new H<sub>2</sub>S sensor technology, it is imperative to fully understand the target applications (including environmental factors, user interface issues, and regulatory requirements) prior to committing to the sensor housing and associated circuitry. During the Phase I, these applications were investigated to further understand their monitoring requirements and any limitations placed on either the sensor or its housing by the operational environment.

## 7.3 PHASE I RESULTS

### 7.3.1 Preparation of Sensing Elements

#### Multilayer Fabrication

Initially, a ceramic tape formulation was developed for use in the fabrication of the multilayer elements. In this work, the relative concentrations of the ceramic raw materials, binder, plasticizer, dispersant, and solvent were optimized. Each of these materials has a unique function in the

process, and thus the appropriate quantities must be determined to ensure that the tape system can be used to successfully produce multilayer sensors.

Once the slip formulations were developed, sensor devices were produced using a multilayer tape casting process [15-16]. Figure 4 shows a flow diagram outlining the steps of the fabrication process. In this procedure, the ceramic powder was first dispersed in an organic solvent using a dispersant. The resulting slurry was then milled to break up any powder agglomerates and to fully disperse the ceramic powders. Next, a binder and a plasticizer were introduced to the dispersion, and the slip was ball-milled for an additional length of time to completely dissolve these materials in the solvent.

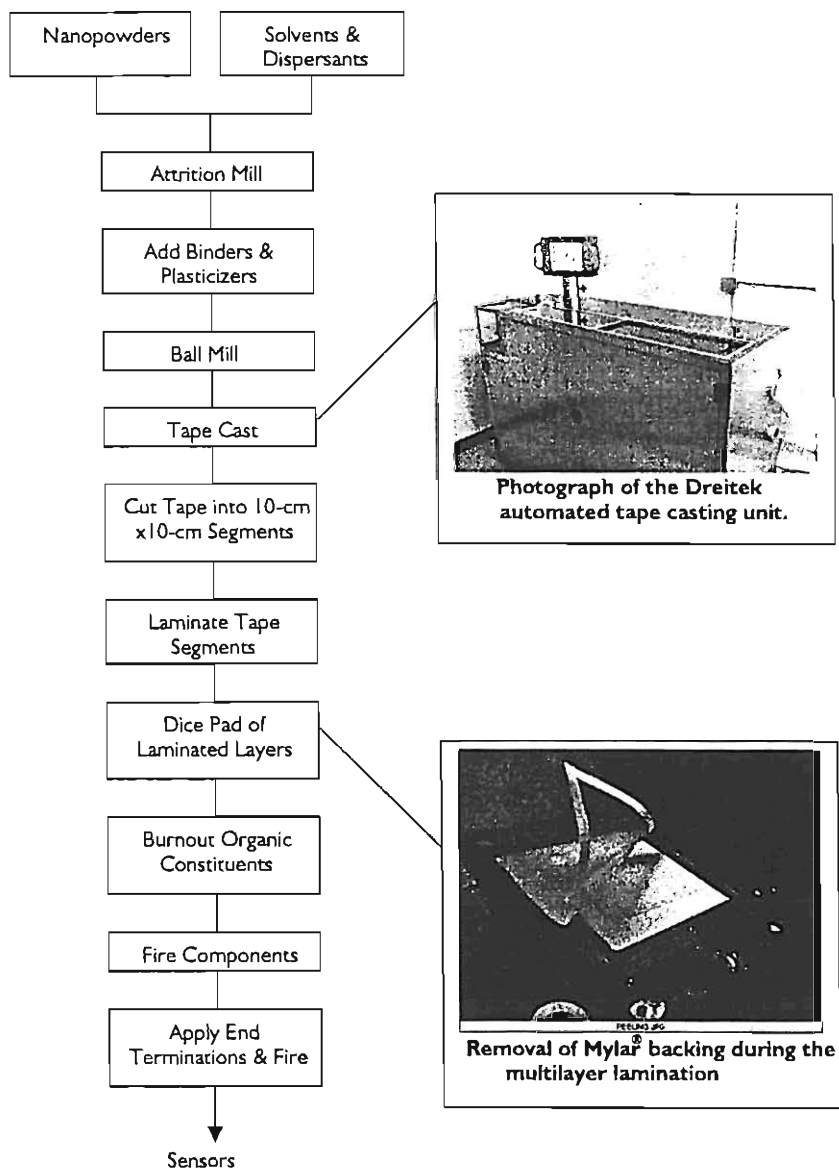


Figure 4. Flow diagram showing the multilayer sensor fabrication process.

The slip was cast using a Dreitek model 101 tape casting unit onto a silicone-coated Mylar® carrier film in a continuous operation in which 10-cm wide tape was produced. As the tape was cast on the Mylar® film, it was dried and rolled onto spools for later use. The cast tape was then cut into 10-cm x 10-cm sheets for use in the multilayer fabrication process. Ceramic devices were fabricated by laminating the various layers together and removing the Mylar® backing after each lamination step. Figure 4 shows an intermediate step in the lamination process in which the Mylar® backing is being removed from an array of devices.

Once the 10-cm x 10-cm multilayer build-up was complete, the array was diced in accordance with the device design. In this work, each ceramic layer had a nominal thickness of 24  $\mu\text{m}$ . Devices with thicker layers were also produced by integrating additional blank (i.e., un-printed) layers into the multilayer structure.

Table 2 summarizes the various multilayer sensor designs that were fabricated during the Phase I project. Sensor compositions containing both tungsten oxide ( $\text{WO}_3$ ) and indium tin oxide (ITO) were utilized for the Phase I devices. For each sensor material, a design using eight layers was used to establish the properties of each composition. In later studies, the indium tin oxide (ITO) was removed from the sensor composition, and the resulting devices exhibited a very low resistance value that was difficult to characterize with the existing test equipment. Therefore, these sensors were re-designed and fabricated using a single, 192- $\mu\text{m}$  thick, active layer. These devices possessed a higher resistance value that was more compatible with the test apparatus.

**Table 2. Summary of multilayer sensor designs produced during Phase I.**

Sensor Composition	Number of Layers	Layer thickness ( $\mu\text{m}$ )
75/25 $\text{WO}_3$ /ITO	8	24
80/20 $\text{WO}_3$ /ITO	8	24
85/15 $\text{WO}_3$ /ITO	8	24
100/0 $\text{WO}_3$ /ITO	8	24
100/0 $\text{WO}_3$ /ITO	1	192

### Thermal Processing and Ceramic Microstructure

After the multilayer sensors were diced into individual components, the organic materials were removed using a low-temperature burnout process. In this procedure, the materials were heated in flowing nitrogen to a maximum temperature of 550°C using a series of ramps and holds. As seen in Figure 5, slow heating rates (0.5 and 1°C/minute) were used, with 50-minute intermediate soaks at 250, 300, 350, 400, 450, and 500°C. Finally, the parts were held at a peak temperature of 550°C for 4 hours. At the conclusion of the burnout profile, the parts were cooled to room temperature at -6°C/minute. The slow heating rate used in this work uniformly removed the organic materials from the multilayer parts. This profile is typical of that used in the manufacture of other multilayer ceramic devices.

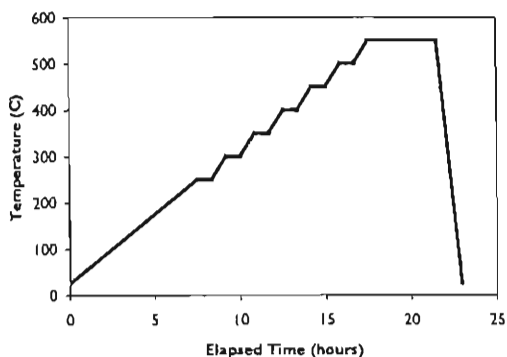


**Figure 5. Thermal profile used to remove the organic materials from the tape cast parts.**

temperatures greater than 1050°C were beginning to melt and deform. Therefore, only the sensor response of the  $WO_3$ /ITO parts fired at 1000°C was measured.

As previously stated, one of the original project goals was to prepare specimens with different degrees of porosity to evaluate the effect of microstructure on mechanical integrity and gas sensor response. During these initial studies, the available window for reliable heat treatment of the  $WO_3$ /ITO parts was too small to allow for the variations in the thermal profile that are necessary to generate different microstructure characteristics.

In the original work performed with this composition (prior to the submission of the Phase I proposal), the ITO was added to promote low-temperature sintering of  $WO_3$ . In the case of thick film devices, the ceramic substrate provides structural support for the porous sensor film. Without this support, the multilayer sensors must be more robust, thereby requiring a greater degree of densification. At the processing temperatures employed, it is likely that the ITO material undergoes significant melting, creating a glassy phase in the grain boundaries of the  $WO_3$  matrix and promoting rapid densification and growth of the  $WO_3$  grains.

To determine if the ITO additives are still required when the parts are prepared in a multilayer configuration, elements were fabricated without ITO and fired at temperatures ranging from 950 to 1125°C. In this case, the materials did not exhibit a tendency to melt at the elevated temperatures, and sensors were successfully processed at various temperatures. The porosity of the materials was measured using an Archimedes technique, and, as seen in Table 3, the resulting materials possessed porosity values ranging from 3% to 50%. It should be noted that the actual temperatures inside the furnace were monitored and those values are reported as the actual temperature (as compared to the set point temperature, which was established with the furnace controller). Figure 7 shows typical examples of the ceramic microstructures obtained when the sensors were fired at temperatures ranging from 975 to 1125°C.

After binder removal, the components were fired to higher temperatures to densify or “sinter” the ceramic sensor material. In this procedure, the devices were heated and cooled to the peak temperature at  $\pm 15^\circ\text{C}/\text{minute}$ . A soak time of 120 minutes at the peak temperature was typically used (see Figure 6).

Initially, sensor devices were produced using  $WO_3$ /ITO ratios of 85/15, 80/20, and 75/25. The resulting components were then fired at temperatures of 950, 1000, 1050, and 1100°C. The best results were obtained when a firing temperature of 1000°C was used. The parts fired at lower temperatures exhibited little mechanical strength, whereas the parts fired at

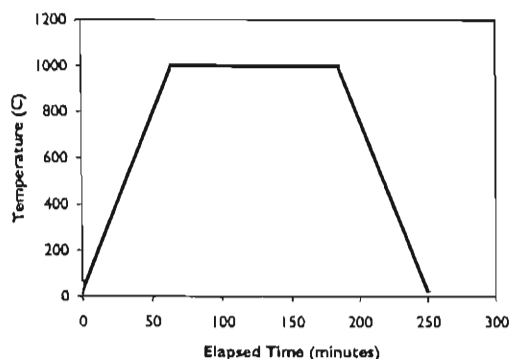


**Figure 6. Typical example of the firing profile used to sinter the  $WO_3$ /ITO multilayers.**

Table 3. Porosity of WO<sub>3</sub> multilayers fired at temperatures from 975 to 1125°C.

Target Temperature (°C)	Actual Temperature (°C)	Apparent Porosity (%)
975	961	49.5
1000	999	47.8
1025	1030	43.3
1050	1038	40.2
1075	1068	29.7
1100	1085	13.7
1125	1120	2.9

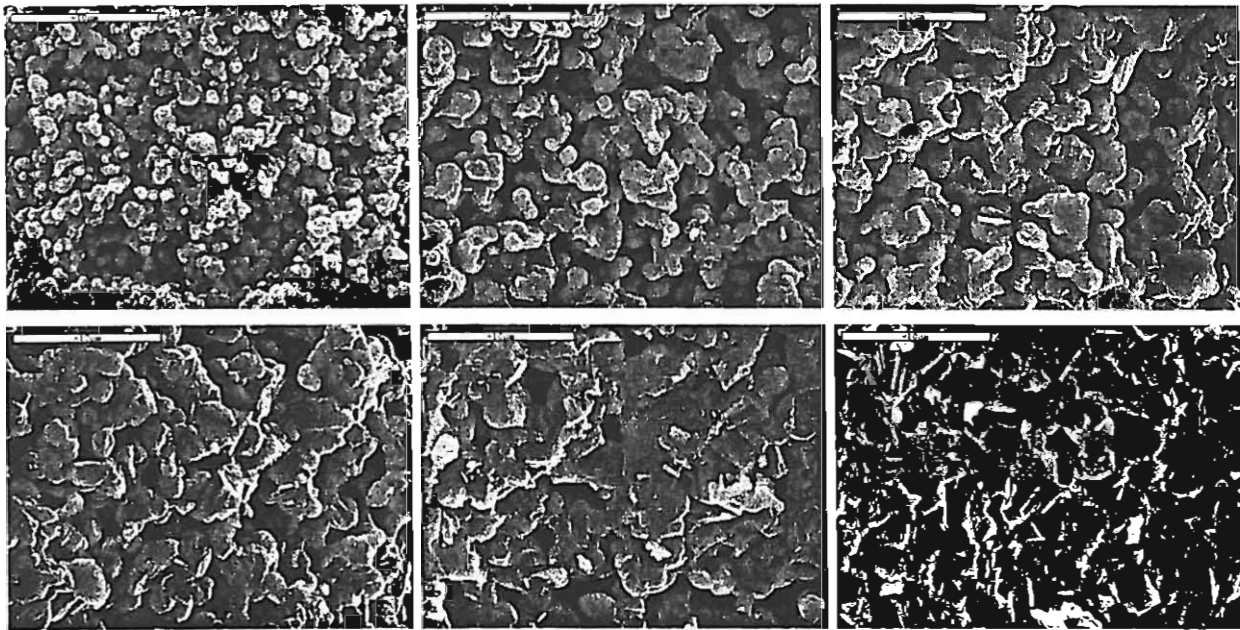


Figure 7. SEM micrographs showing the decreasing porosity obtained as the sintering temperature is increased. The above images were obtained from specimens fired at 975°C (upper left), 1025°C (upper middle), 1050°C (upper right), 1075°C (lower left), 1100°C (lower center), and 1125°C (lower right).

### 7.3.2 Characterization of Sensing Elements

#### Measurement System

Measurement of the gas response of the multilayer sensors was accomplished by determining the change in each device's electrical resistance in the presence of toxic gases. Testing was carried out using Nanomaterials Research's hazardous gas test system. This system is one of the newest test stations established by Nanomaterials and features a custom-designed heated test block, custom circuitry for sensor output measurement, and mass flow controllers for gas mixing. All of the components are linked together through a LabView program that enables the user to input the

desired sensor operating temperature, gas flow rate, and gas introduction schedule. Because of the toxic nature of the gases employed with this test station, the entire gas mixing and delivery system is contained in a fume hood to prevent accidental user exposure to the gases under test.

The test system (illustrated in Figure 8) consists of control and measurement electronics located in a 19" rack, with test fixtures sized to be located in the fume hood. The test fixtures incorporate a common base structure containing mass flow controllers for gas mixing. Separate testing beds for sensor elements and packaged sensors may be attached to the base fixture, each with separate, but compatible, electrical interconnections. This design minimizes costs, while allowing the flexibility to test both sensor elements and packaged sensors.

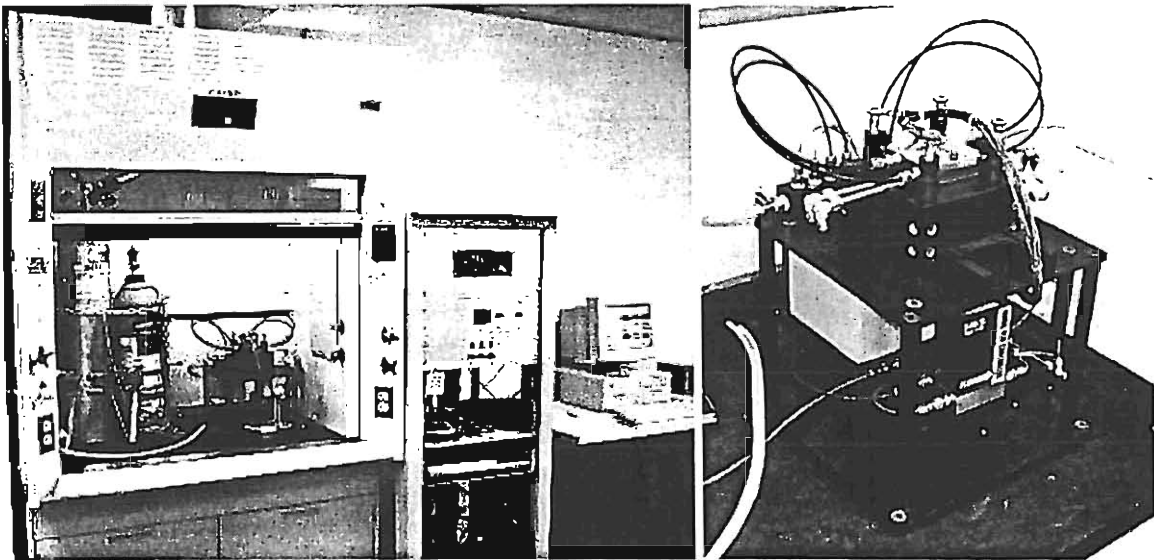


Figure 8. Photographs showing the hazardous gas test system in a fume hood (left) and a close-up image of the test apparatus (right).

The sensor element test fixture consists of a clamshell-type stainless steel chamber that can be both heated and cooled by external means (cartridge heaters/liquid coolant) and allows control of the chamber's atmosphere via gas flow at ambient pressure. The bottom portion of the chamber contains a recess that can hold a 3 x 3 array of sensor elements. Electrical contacts to the sensor elements are made via spring-loaded "pogo pin" connectors.

Test gases are supplied in the desired concentrations using two mass flow controllers operated in combination. In the case of H<sub>2</sub>S testing, a 100-ppm gas cylinder containing hydrogen sulfide diluted in nitrogen was mixed with a cylinder of dry air to attain the different concentrations required for linearity testing.

During the Phase I project, a simplified data acquisition set-up was established in order to facilitate automated testing during the 6-month project. This system is operated from a power supply that applied 5V to nine separate voltage divider circuits, which incorporate the nine sensors from the sensor test head. A LabView program was written to automate a number of functions. These included switching of gas flows (mixing of hydrogen sulfide in nitrogen and air) at specified times; acquiring voltage readings from each voltage divider; calculating sensor resistances; and recording the resistance along with the time that each measurement was made (usually every second). The

resulting data is exported to an Excel spreadsheet for data analysis. This set-up has been quite useful in allowing us to test multiple sensors simultaneously.

Unfortunately, this test circuitry was originally designed for sensors with resistances of  $10^3$  to  $10^8$  ohms, which is typical of the planar (i.e., thick film) resistive sensors developed and sold by Nanomaterials Research. However, in this work, the resistance values for several of the multilayer devices were found to be considerably lower, requiring us to make a few adjustments in order to prevent overheating of both the sensors and the circuit components. To limit overheating of the circuitry, larger surface area cooling fins for heat dissipation were added to the circuit, and the testing was limited to less than five sensors at a time.

However, self-heating issues related to the individual sensors proved to be a more intractable problem. The initial multilayer sensors produced without ITO exhibited resistance values from 1-5 k $\Omega$  at ambient temperatures. However, when the sensors were heated for operation (to temperatures of 100, 200, and 300°C), the baseline resistance in air dropped off considerably (to below 20  $\Omega$  when exposed to gas at 200°C for some sensors). The multilayer architecture was then redesigned to increase resistance, allowing better measurement of sensor response. However, when these devices were processed at higher temperatures to promote densification, the resistance was again found to decrease significantly, bringing the sensors back into the low resistance range that proved difficult with the current test arrangement.

For measurements in which the samples exhibited the lowest resistances (~15 ohms), the application of the system's 5V input signal led to a considerable current and power draw (>1.5W), which was sufficient to potentially cause self-heating of the sensors. At the more typical resistances of 60-100 ohms, the resultant power draw was less than 0.4W, which is less likely to cause significant problems. In certain cases, it was found to be necessary to decrease the voltage input to the sensors to 2V in order to minimize the self-heating of the lowest resistance sensors.

The resulting data served to establish the magnitude of the gas response and the recovery and linearity characteristics for the different sensor elements produced. However, the possibility of self-heating during certain measurements, may have complicated comparisons among the different samples. This issue will be further addressed during the Phase II program. The associated circuitry will be redesigned to provide a sufficiently low input voltage as to avoid self-heating even during elevated temperature testing of very low resistance components. In addition, steps will be taken to redesign the internal electrode structure of the components to further increase device resistance. Finally, additives with high resistance may be incorporated into the sensor matrix, followed by extensive testing to ensure that the additions do not compromise the sensor response. In this manner, we can ensure that the microstructure of the sensor devices is optimized to enable maximum response to gas.

### Response of Sensors Containing ITO Additions

The initial multilayer devices contained eight, single-stacked layers and were fabricated using 85/15, 80/20, and 75/25 WO<sub>3</sub>/ITO compositions and Pt internal electrodes. The sensors fabricated from the 85/15 material had room-temperature resistance values on the order of 30 k $\Omega$ , and these sensors were tested extensively.

As seen in Table 4, the sensors showed an increasing response to H<sub>2</sub>S as the parts were heated from 25 to 200°C. As expected, the resistance in air decreased as the sensor elements were heated. This behavior is typical of n-type ceramic semiconductors.

Table 4. Typical response of prototype multilayer sensors (lot number H2S-AB-313-01) to 20 ppm H<sub>2</sub>S at 25, 50, 100, and 200°C.

Temperature (°C)	R <sub>a</sub> (kΩ)	R <sub>g</sub> (kΩ)	R <sub>a</sub> /R <sub>g</sub>
25	3.90	3.81	1.02
50	2.63	2.41	1.09
100	0.94	0.75	1.25
200	0.47	0.20	2.37

When exposed to 20 ppm H<sub>2</sub>S in air, the sensors exhibited negligible responses at 25 and 50°C, but exhibited a strong response ( $R_a/R_g = 2.37$ ) at 200°C. A representative measurement of the change in resistance in response to gas introduction for four sensor devices is shown in Figure 9. Under these conditions, the resistance decreased from approximately 450 Ω to 200 Ω when exposed to the test gas. However, the resistance did continue to decrease slightly as the exposure continued for 600 seconds, indicating that the surface reactions were incomplete.

Furthermore, while these sensors showed a rapid decrease in resistance upon initial exposure to the test gas, the resistance value did not return to the pre-exposure value after the gas was removed. This result suggests that some H<sub>2</sub>S remained on the surface of the sensor, causing the resistance to remain low even after the gas was removed from the environment (at 900 seconds). While the response to gas was very good for these devices, the retention of H<sub>2</sub>S and other sulfur-containing gases often poses a problem for metal oxide sensors. Typically, the composition of the sensors is modified in an effort to improve sensor recovery. Other options include pulsed heating, flushing of the system with a neutral gas, or recalibration.

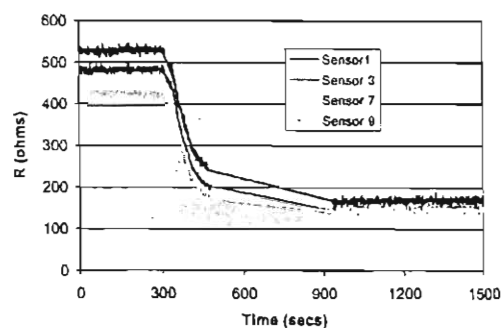


Figure 9. Typical response of 85/15 WO<sub>3</sub>/ITO multilayer sensors to 20 ppm H<sub>2</sub>S at 200°C (lot number AB-313-01b).

### Effect of Sensor Composition

Removal of the ITO from the sensor composition led to considerable improvement in both sensor response and recovery. Initially, WO<sub>3</sub> multilayer components were produced using the same design as previously used (i.e., eight active internal layers with Pt internal electrodes). These devices exhibited a much stronger response to the presence of H<sub>2</sub>S than the WO<sub>3</sub>/ITO composite materials. Figure 10 shows the response for a typical sensor to 20 ppm at 300°C. The magnitude of the response (i.e.,  $R_a/R_g$ ) was nearly double that observed for the specimens containing ITO. In addition, the sensors recovered significantly after exposure to gas, returning to approximately 60-70% of their original baseline in air after the first exposure to H<sub>2</sub>S. This result was particularly

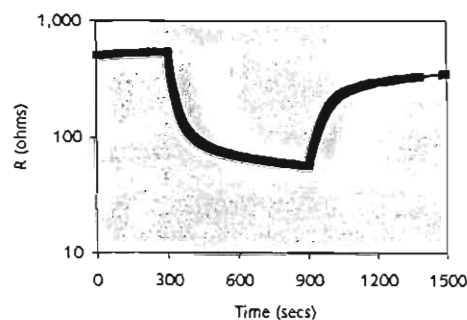


Figure 10. Response to 20 ppm H<sub>2</sub>S for a typical WO<sub>3</sub> sensor operated at 300°C.

encouraging given the complete lack of recovery for the devices containing ITO.

Cyclic exposure testing was then performed, during which the sensors were repeatedly exposed to either 20-ppm H<sub>2</sub>S or dry air for 5-minute cycles. A typical plot of sensor response to repeated exposures is provided in Figure 11. It should be noted that the magnitude of the gas response was greatest during initial exposure, but recovery was incomplete. However, the repeatability of the response characteristics improved dramatically after the initial exposure, with R<sub>a</sub>/R<sub>g</sub> varying by less than 10% after the third exposure. Moreover, the recovery improved in a similar fashion, with less than 6% variation between the initial and final resistance values in air. These results suggest that the sensor can be sufficiently calibrated in the laboratory in order to achieve very good repeatability during operation.

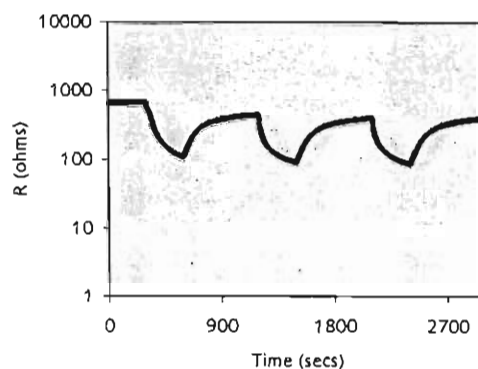


Figure 11. Typical response to repeated exposures to 20 ppm H<sub>2</sub>S.

Next, the linearity of the sensor response with gas concentration was evaluated. The sensors were exposed to concentrations of 5, 10, 20, and 50 ppm H<sub>2</sub>S, and the magnitude of the gas response was monitored. Figure 12 compares the responses of five individual WO<sub>3</sub> multilayer sensors under the various test conditions. The sensors were found to exhibit good linearity over the entire concentration range of interest (5-50 ppm), indicating that the devices can be successfully operated for quantitative real-time exposure monitoring at levels of interest to the industrial hygiene community.

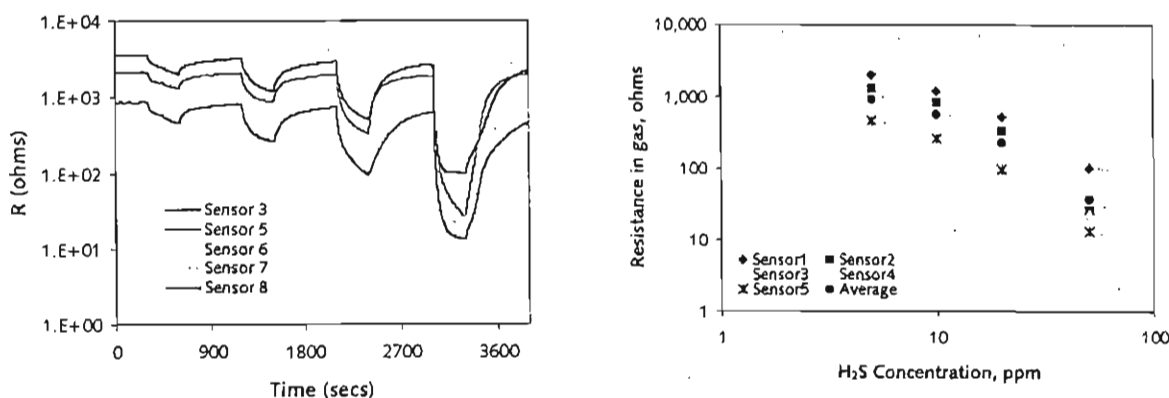


Figure 12. Effect of different H<sub>2</sub>S concentrations on WO<sub>3</sub> sensor response when operated at 300°C.

### Effect of Pad Design

As previously discussed, the multilayer fabrication process provides considerable benefits with respect to tailoring the electrical properties of sensor components. For example, the internal electrode configuration and geometry of the different layers can be redesigned to increase or decrease the baseline resistance of the sensors to better meet the requirements of the associated

measurement electronics. This effect is particularly important for a material with very high resistivity, as well a material with very low resistivity (such as the  $\text{WO}_3$  sensors investigated herein).

To demonstrate this advantage, devices were also prepared with only one large internal layer (see Figure 13) to determine the differences in resistance behavior. As anticipated, the resulting devices were found to exhibit higher average resistance values at all temperatures tested. For example, when tested at 100°C in dry air, devices prepared with eight active layers exhibited average resistances of around 200  $\Omega$ . In contrast, devices prepared with one active layer exhibited average resistances around 5000  $\Omega$  at the same conditions.

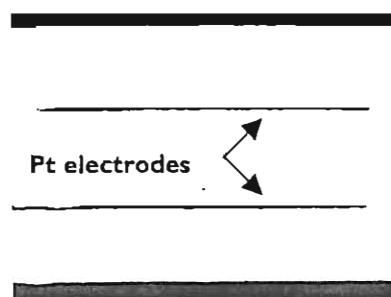


**Figure 13. Optical microscope image of a  $\text{WO}_3$  multilayer with one active internal layer.**

More importantly, however, the devices produced using the second pad design were found to exhibit even better response to gas than the previously prepared components. The components demonstrated on average a 12X response to the presence of 20-ppm  $\text{H}_2\text{S}$  when operated at 200°C. In addition, the sensors were found to recover completely after gas exposure if heated to 300°C, although the magnitude of the response at 300°C was somewhat lower (average of 2.8X). Results for a typical component are shown in Figure 14, and the response and recovery data are tabulated in Table 5.

These data indicate that it is conceivable to operate the sensor at lower temperatures to perform sensitive measurements, particularly at very low concentrations such as 5 ppm or less). In addition, the sensor can be heated to higher temperatures to promote complete removal of the gas from the sensor surface. This result leads to the possible application of controlled pulse heating of the sensor device, which will be explored extensively during the Phase II program. Pulse operating modes have additional benefits in terms of power consumption and optimization of response that will be important for small, battery-operated personal monitor applications.

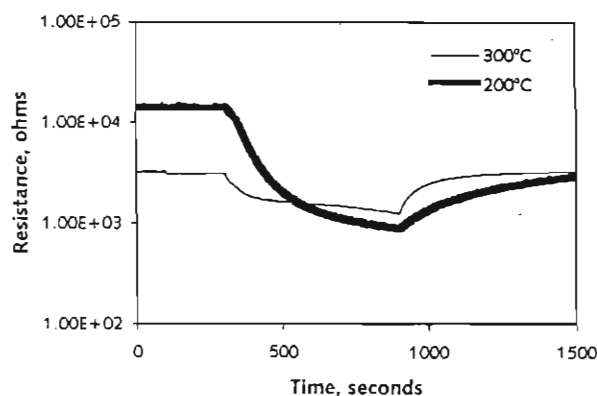


**Figure 14. Response of a typical  $\text{WO}_3$  sensor produced with only one active layer. Sensor was exposed to 20 ppm  $\text{H}_2\text{S}$  in dry air at both 200 and 300°C.**

**Table 5. Effect of operating temperature on response and recovery of a typical batch of  $\text{WO}_3$  multilayer sensors containing one active internal layer. Each data point represents the average of five sensors tested simultaneously.**

	100°C	200°C	300°C
Response	1.97	11.78	2.78
Recovery	53.79%	20.15%	101.24%

### Effect of Starting Particle Size

In addition to pad design, the particle size of the starting  $\text{WO}_3$  powder was also found to affect the response characteristics of the sensor components, in particular the magnitude of the response at a given temperature. Tungsten oxide powder was purchased from the manufacturer with a starting average particle diameter of approximately  $0.5\ \mu\text{m}$ . Attrition milling was then used to break up the material, reducing the particle size to approximately  $60\ \text{nm}$ . This material was then employed as the starting powder for building pads with and without ITO and with different active layer counts.

The as-received powder was also milled for a slightly shorter period, resulting in a material with an average particle size of only  $\sim 80\ \text{nm}$ . The characteristics for the different milled lots are reported in Table 6. The  $80\text{-nm}$  powder was also used to prepare components with one active layer for comparison. The diced parts were heat treated in the same manner as the previously prepared components, and the resulting responses to  $20\text{-ppm}\ \text{H}_2\text{S}$  were determined over an operating temperature range from  $100$  to  $300^\circ\text{C}$ .

Figure 15 compares the responses of two components, each of which was prepared from a different batch of the milled powder. As seen in the figure, the components fabricated from the finer powder demonstrated a larger response to gas ( $\sim 12\text{X}$  at  $200^\circ\text{C}$ ), with similar recovery characteristics (20-30%). At  $300^\circ\text{C}$ , components produced from the  $60\text{-nm}$  powder demonstrated an average response of  $2.8\text{X}$ , with full recovery, while similar components produced from  $80\text{-nm}$  powder demonstrated only a  $1.7\text{X}$  response and 96% recovery on average.

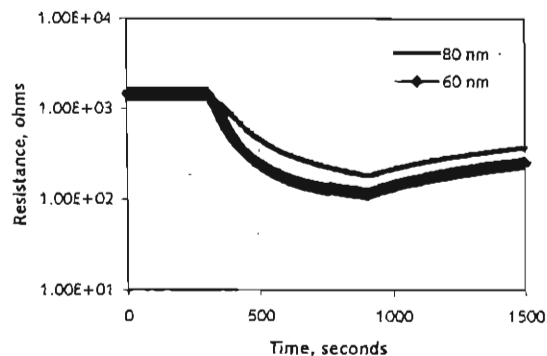


Figure 15. Responses to  $20\ \text{ppm}\ \text{H}_2\text{S}$  for components prepared from different powders.

Table 6. Powder characteristics for the different  $\text{WO}_3$  materials. All materials were prepared from the same lot of powder received from the vendor.

	Specific Surface Area ( $\text{m}^2/\text{g}$ )	Average Particle Diameter (nm)
As-received	1.5	558.65
Milling 1	14.0	59.86
Milling 2	10.3	81.36

### Effect of Porosity

The previous results confirm that the starting particle size plays a significant role in the optimization of gas sensor response. Further investigation of this effect will be included in the Phase II work plan. However, variation in sensor response may also be related to the degree of open porosity in the device structure, which can affect gas diffusion to the surface of the individual grains. To

provide a preliminary look at this effect, components were processed using different thermal profiles to reduce open porosity. It should be noted, however, that increasing the processing temperature can also lead to grain growth in the ceramic layer, increasing the final grain size. This secondary effect was not taken into account during these preliminary Phase I trials but will be included in the Phase II follow-on investigations.

To generate different degrees of porosity, components fabricated from the 80-nm powder were heated to different peak temperatures (950 to 1125°C). The resulting multilayer devices were found to possess microstructures with porosity values ranging from near 50% (when processed at the lowest temperature) to less than 3% (when processed at the highest temperature). The resistance of each of the sensors was monitored at both 200 and 250°C, and the devices were exposed to 20 ppm H<sub>2</sub>S for 10 minutes at each temperature.

The resistance of the sensor devices in air was found to decrease significantly with increasing processing temperature. For example, devices heated to 1000°C exhibited average resistances over 1100 Ω at 200°C, while devices processed at 1125°C exhibited resistances closer to 50 Ω at the same temperature. This result indicates that as the open porosity is reduced during densification, contact between grains is increased, and the conductive nature of the tungsten oxide material begins to dominate.

In addition to variations in resistance, the response of the sensors to H<sub>2</sub>S was also found to vary with processing temperature, with maximum response occurring for devices processed at 1000°C. The effect of processing temperature is illustrated in Figure 16 in which the sensor response is plotted along with the average porosity values for the different components. Devices processed at 1000°C demonstrated average responses of 5-6X when exposed to the challenge gas, which were

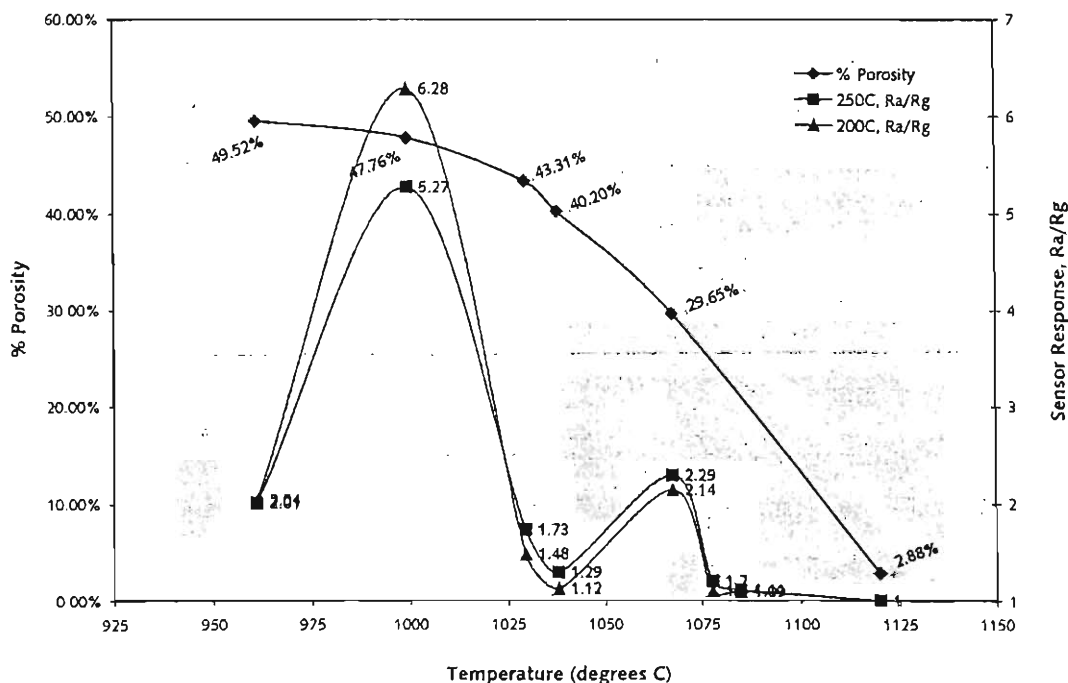


Figure 16. Effect of processing temperature on gas response.

in line with the previously obtained results. However, devices processed at 1125°C exhibited responses of only 1.1X. Furthermore, the results were non-linear with processing temperature, and a slight increase in response was found at 1075° (~2.3X), indicating that the resistance behavior is a complex function and other variables may contribute significantly.

As previously discussed, the electrical behavior of metal oxide semiconductors is influenced by a number of factors. During testing, resistance was monitored as a function of both operating temperature and gas atmosphere. In addition, devices with different average grain sizes and degrees of porosity were prepared. However, two other significant variables may also contribute to gas sensor response for this material. These include crystalline phase and degree of oxidation. Tungsten oxide ( $\text{WO}_3$ ) is known to exist in four distinct crystal structures, namely triclinic, monoclinic, orthorhombic, and tetragonal. In particular, the orthorhombic and tetragonal phases are likely to be formed at temperatures near those employed in this program, and the possibility exists for formation of multiple phases simultaneously. In previous studies, these phases have been found to exhibit different kinetic energies for oxygen release and pickup, as well as different conductivity values [17]. In addition, tungsten can be present in the lattice structure as  $\text{W}^{6+}$ ,  $\text{W}^{5+}$ , or  $\text{W}^{4+}$  (or a mixture) depending on the atmospheric conditions present at elevated temperatures. Furthermore, the electrical conductivity has been found to decrease with increasing oxygen content, indicating that the highly conductive specimens produced at high temperatures may contain a greater fraction of oxygen vacancies, which can affect gas response.

The Phase I results confirmed that optimization of sensor response is a complex issue in which a number of variables must be evaluated in concert. Effects due to operating temperature, grain size, and porosity were clearly identified. In addition, potential effects due to crystalline structure changes and oxidation state were found, which will require more extensive study during the Phase II program. The Phase I sensors demonstrated large, repeatable and linear responses to  $\text{H}_2\text{S}$  vapors. In addition, the multilayer components possessed the mechanical strength necessary for routine handling, mounting, and integration into the test apparatus, an issue of chief concern at the start of the Phase I. Continued experimentation will be pursued to provide further information regarding device optimization to ensure rapid commercialization of the technology.

#### 7.4 COMMERCIALIZATION POTENTIAL

As previously discussed, hydrogen sulfide is widely used in a number of industries. It is a major component in the production of elemental sulfur and sulfuric acid. It is also used in the manufacture of heavy water for the nuclear industry and in the production of sodium sulfide and various thiophenes. It is a component in rayon manufacturing and is used as an agricultural disinfectant, as a reagent in analytical chemistry, and as an additive in lubricants. It is also a routinely produced byproduct of pulp and paper manufacturing.

In addition to direct contact with hydrogen sulfide during manufacturing operations, concerns exist regarding the emission of  $\text{H}_2\text{S}$  vapors into the atmosphere. The majority of atmospheric hydrogen sulfide (~90%) is derived from natural sources including volcanoes, some plant species, the ocean, and stagnant water with low oxygen content (e.g., bogs and swamps). In addition,  $\text{H}_2\text{S}$  emissions are commonly associated with sewers, septic tanks, livestock waste pits, manholes, well pits, landfills, and wastewater treatment plants.

Hydrogen sulfide gas also occurs naturally in petroleum and natural gas (which can contain up to 28%  $\text{H}_2\text{S}$  depending on its source). Significant  $\text{H}_2\text{S}$  emissions can be found near natural gas production areas and at petroleum refineries, and the oil and gas industry remains among the most

heavily regulated for workplace exposure to H<sub>2</sub>S vapor. About 4 million tons of sulfur are recovered in the U.S. each year from natural gas and petroleum refinery gases.

While a much smaller source, it should also be noted that some bacteria can change calcium sulfate, the primary constituent of wallboard, into H<sub>2</sub>S. If construction and demolition debris contain large quantities of wallboard, H<sub>2</sub>S emissions can be quite large. The threat is greatest if the wallboard is finely crushed and little oxygen is present (e.g., if buried in a landfill).

The toxicity of hydrogen sulfide (H<sub>2</sub>S) is similar to that of cyanide. It reacts with the enzymes in the blood that inhibit cell respiration and, at high concentrations, can literally shut off the lungs. Eighty fatalities related to H<sub>2</sub>S exposure were reported in the US between 1984 and 1994, fourteen of which involved attempted rescuers [18]. The majority of these deaths (77%) were in businesses with more than 11 employees, which were, therefore, subject to routine OSHA inspections. The fatalities were primarily associated with confined space operations (e.g., sewers, animal containment facilities, waste dumps, sludge plants, manure tanks, and cesspools) and the petroleum and natural gas industries. OSHA has determined that the use of H<sub>2</sub>S detection equipment, coupled with better availability of air-supplied respirators and additional confined space training, may have potentially prevented deaths in the vast majority of these cases.

Occupations and related facilities with the greatest risk of worker exposure include:

- **Agriculture** – livestock farms, animal fat and oil processing plants, manure removal operations, fertilizer storage facilities, slaughterhouses, and sugar beet and cane farms
- **Chemical processing** – breweries and fermentation facilities; plants for producing barium carbonate, barium salts, bromide-brine solutions, carbon disulfide, purified hydrochloric acid, purified phosphates, sulfur products, and thiophenes.
- **Construction** – sulfur-containing asphalt paving operations, cable splicing operations, excavations, underground tunnels, and painting operations
- **Electronics assembly** – lithographers and photoengravers
- **Manufacturing** – manufacturing facilities for pulp and paper, artificial flavors, cellophane, depilatory solutions, dyes, felts, fertilizer, glue, rayon, refrigerants, rubber, plastics, silk, soap, synthetic fibers, and textiles
- **Metal processing** – facilities using blast furnaces, coke and coal ovens, and equipment for removing sulfur from copper- or lead-ore; geothermal power drilling and production operations; gold-ore processing facilities; mines; and smelting operations
- **Nuclear power** – heavy water manufacturing plants
- **Oil and gas** – natural gas production and processing facilities, petroleum production and refining operations, and pipelines
- **Wastewater treatment** – landfills, manholes and trenches, septic tanks, sewage treatment plants, sewers, and wells

In general, the threat is greatest for confined space workers, who are routinely exposed to oxygen-deficient, toxic, or flammable atmospheres. More than 60% of confined space fatalities occur among rescuers, indicating that such individuals should be well-trained in monitoring equipment, personal protective equipment, and proper procedures for confined space entry. Examples of

confined spaces include storage tanks, compartments of ships, process and reaction vessels, septic tanks, sewage digesters, pumping and lift stations, sewage distribution/holding tanks, silos, vats, ventilation and exhaust ducts, underground utility vaults, tunnels, boilers, pipelines, and pits. Such spaces should be adequately tested before entry to determine the presence of toxic species, the oxygen level present, and the potential for flammability.

For example, OSHA requires all sewer crews to have on hand a gas detector to measure atmospheric gases in the manhole prior to removal of the lid. Monitoring must include explosive gases, oxygen, and hydrogen sulfide.  $H_2S$  is generated in the flow when sewage is allowed to stand for long periods, becoming stagnant or septic. In these anaerobic conditions, the sewage can easily contain up to 6000 ppm  $H_2S$  [19]. Although  $H_2S$  is normally heavier than air, it can be released at dangerously high levels if a plug is removed or a pump is turned on.

As part of the Phase I program, Nanomaterials Research identified three specific markets where the need for improved  $H_2S$  sensors and related instrumentation is particularly important. These include the oil and gas industry, wastewater treatment, and agriculture. Each will now be briefly discussed.

### Oil & Gas

Hydrogen sulfide is routinely brought to the surface from wells drilled for natural gas, particularly in certain geographic areas. For example,  $H_2S$  release is common in the mile-deep, energy-bearing Niagaran Salina formation in northern Michigan. Deliberate and accidental releases of  $H_2S$  from wells in this area have led to numerous documented injuries, emergency evacuations, and livestock deaths. Since 1980, at least 10 separate accidental releases have occurred requiring the evacuation of over 260 people from their homes. Since 1994, at least 22 people, four of them children, have been seriously injured by such releases, requiring hospital treatment. In addition, at least 35 head of cattle have been killed by toxic gas exposure.

Due to these releases, public concern in residential areas close to where oil and gas development occurs is high. For example, in a typical year, the Michigan Department of Environmental Quality (MDEQ) receives approximately 20 odor complaints, the majority of which can be attributed to  $H_2S$  release near oil and gas operations.

The potential for release of life-threatening concentrations of  $H_2S$  from "sour" oil and gas operations is well known. Employers involved in the transport of sour crude oils from production well sites to pipelines are required to manually gauge storage tanks before and after each transfer in accordance with procedures established by the American Petroleum Institute. As these tanks are located outside and in remote locations, employees are dispatched on a regular basis for testing. Gauging requires the employee to climb to the top of the tank, open a thief hatch, and determine the tank level via a plumb bob. Exposure to  $H_2S$  can occur when the hatch is open, and potentially several hundred parts per million concentrations can be present in the vapor space of the tank. In addition, a recent report [20] indicated that liquid phase  $H_2S$  concentrations above 8 ppm by weight can produce atmospheres that are immediately dangerous to life or health (IDLH) in residual fuel oil storage tanks and ship and barge holds.

Sensor and instrumentation needs within this industry vary considerably. Hand-held monitoring instruments are widely used to sample the atmosphere within tanks and pipes prior to opening. In addition, personal "badge-style" monitors are needed to directly protect personnel near such openings. Although colorimetric badges are currently available, a quantitative analysis method, with alarm capabilities, would offer significantly greater protection. Finally, stationary systems are

used, although infrequently, at certain pipeline locations where the potential for widespread exposure is greatest.

### Agriculture

Hazardous atmospheres exist in many agricultural confined spaces. For example, manure storage facilities may contain methane, H<sub>2</sub>S, CO<sub>2</sub>, and NH<sub>3</sub>. From 1980 to 1989, at least 48 workers died from toxic gas exposure. In addition, it is estimated that several thousand workers suffer chronic and acute health effects related to lower level exposure on a regular basis. In May 1990, NIOSH issued an Alert regarding the dangers associated with manure pits [21]. This alert described seven deaths from asphyxiation that occurred during two incidents involving entry into manure pits.

Of the approximately 2.3M farms in the US (based on 1985 USDA estimates), a large fraction may contain manure pits or tanks. Such systems are used primarily on livestock farms (including dairy operations) to allow for easier cleaning of animal confinement areas and efficient underground storage of raw waste. Inside the pit, the manure undergoes anaerobic digestive fermentation to form fertilizer, generating CH<sub>4</sub>, CO<sub>2</sub>, NH<sub>3</sub>, and H<sub>2</sub>S. The accumulation of gases within the confined space can produce an oxygen-deficient, toxic, and potentially explosive environment.

No OSHA standards exist for work in and around manure pits. OSHA is reviewing a proposed rule on confined space procedures that would address safety in such areas, but this standard would not be enforced on farms with 10 or fewer workers. NIOSH published criteria for a recommended standard for working in confined spaces in 1979, an alert on confined space hazards in 1986, and a guide for working in confined spaces in 1987. However, many farm workers remain unaware of the immediate danger posed by entry into manure pits. Like other types of confined spaces, manure pits present a special problem as the dangerous conditions may exist only intermittently.

In addition to worker safety, livestock experience prolonged exposure to toxic pollutants including both gases and airborne particulates. Continual exposure can lead to stress, loss of appetite, aggravation of existing diseases, and even death. The result is higher veterinary costs, higher animal mortality, decreased feed efficiency, more days to raise a market animal, and lower quality product. These costs are ultimately passed along to the consumer.

The agriculture market is unique to the gas sensor community in many ways. In contrast to the chemical processing and oil and gas industries, agricultural workers do not regularly use monitoring instrumentation. Therefore, such instruments must be user-friendly, able to operate in harsh operating conditions (e.g., outside temperature and humidity fluctuations), and extremely cost-effective. Most farms require only a stationary monitoring system, placed at the most critical location. Hand-held monitors have potential uses as well, particularly for large farms.

### Wastewater Treatment

H<sub>2</sub>S can form in sewer lines, decaying the underground piping. Often, privately operated lift stations have difficulty maintaining acceptable levels as established by the sanitation district. Typically, the sanitation department performs multi-day monitoring of manholes to establish compliance. Data-logging instruments utilizing electrochemical H<sub>2</sub>S sensors are used for these tests. Such sensors are considered quite accurate and have a life span of 12-18 months under ideal conditions. However, in the humid and sometimes high levels of H<sub>2</sub>S experienced in sewer lines, the life span can end within a matter of hours [22]. This is a costly situation when one considers the labor associated with multi-day monitoring, the cost of a replacement sensor, and the time lost waiting for the instrument to be repaired and re-calibrated. In Nevada, a study was conducted

using a solid-state sensor system manufactured by International Sensor Technology. In field conditions that previously rendered the electrochemical sensors useless, the solid state sensors survived even after hours of exposure to H<sub>2</sub>S levels exceeding 100 ppm. The only maintenance required was normal monthly calibration performed locally.

This market is among the most established for H<sub>2</sub>S instrumentation. Therefore, more information regarding needs for new technology is available. Wastewater treatment workers can benefit particularly from the development and commercialization of new personal exposure monitors both hand-held and badge-style.

### **Spin-off Opportunities in Emission Monitoring for Public Health**

In addition to exposed workers, individuals living near facilities emitting H<sub>2</sub>S are also at risk for adverse health effects. For example, foul odors and health issues were investigated in an Indiana community near a waste disposal lagoon and in five New York communities near landfills containing construction and demolition debris. In Indiana, H<sub>2</sub>S levels of 300 ppb were found during a two-month test period. In New York, the levels reached 4000 ppb over a several-month period. Many members of the communities complained of eye, throat, and lung irritation, nausea, headache, nasal blockage, sleeping difficulties, weight loss, chest pain, and asthma attacks.

Several studies, including surveys in North Carolina and Iowa, have found that people living near hog factories suffer from increased respiratory problems, headaches, diarrhea, and other problems commonly associated with H<sub>2</sub>S exposure [23].

Finally, in 1996, five Finnish researchers profiled two towns, one polluted by a pulp mill (with considerable H<sub>2</sub>S emissions) and one non-industrialized. Residents of the polluted city were found to experience substantially more respiratory infections, headaches, and coughing [24].

Spin-off opportunities in public safety emission monitoring may exist for the technology developed herein. However, it will be necessary to concentrate on ensuring that the detection limit of the sensor is sufficiently low as to ensure that levels of hydrogen sulfide of concern for public air quality can be reliably detected. Currently, the sensor can reliably detect concentrations ranging from 5 to 50 ppm. For this application, levels from 0.1 to 1 ppm must be easily quantified. As the Phase II program progresses, Nanomaterials Research will further evaluate the detection limit of the sensor to determine if this spin-off application is feasible.

## **7.5 PHASE I CONCLUSIONS AND OUTLOOK FOR PHASE II**

This SBIR Phase I program successfully demonstrated a new type of H<sub>2</sub>S sensor device for workplace safety monitoring. This sensor combined advances in fabrication and materials science to create a component that offers reliable detection within the concentration range of 5 to 50 ppm, which is required for industrial health and safety applications of the sensor.

The criteria listed below were identified in the Phase I proposal as essential for demonstration of Phase I feasibility. The following paragraphs detail our success at meeting each of these criteria.

### **1. Fabrication of robust multilayer sensing elements with sufficient mechanical strength for packaging according to conventional electronic component packages.**

The multilayer sensors produced during the Phase I project possessed the requisite mechanical strength needed for handling, mounting, and packaging of the sensors for testing in the company's hazardous gas test system. Integration of the sensors

into the test chamber involved mounting the sensors onto rigid carrier substrates for more easy electrical connection. Components were prepared with 3-50% porosity, all of which were found sufficiently durable for easy handling during the mounting process.

**2. Reproducible detection of 5 to 50 ppm H<sub>2</sub>S with an accuracy of ±10% or 1 ppm, whichever is greater.**

As shown in Figure 12, the sensors prepared during the Phase I project readily detected H<sub>2</sub>S concentrations within the range from 5 to 50 ppm. The sensors exhibited changes in resistance in proportion to the quantity of gas present. Furthermore, the magnitude of the response was sufficiently large as to enable discrimination of intermediate concentrations, clearly demonstrating an accuracy of better than 10% of the measurement range.

**3. Response time of less than 1 minute to challenge gas.**

The sensors rapidly detected the presence of small concentrations of H<sub>2</sub>S, reaching  $t_{50}$  within 20 seconds and  $t_{90}$  within 60-90 seconds. In general, sensors heated to higher temperatures (250-300°C) responded slightly faster, although the magnitude of the response was typically less. A typical example of the sensor response is shown in Figure 11.

While all of the Phase I research goals were successfully met, additional work is required for further development of this technology for transition to the commercial marketplace. That work will likely include the following tasks:

1. Optimizing the composition of the sensor to achieve a maximum response to H<sub>2</sub>S at low temperatures. This work may include the addition of Au catalyst into the sensor as either a dopant to the WO<sub>3</sub> phase or as an internal electrode material.
2. Further evaluating the relationship between porosity, grain size, crystal structure, oxidation state, and sensor response. The Phase I work clearly illustrated that the sensor response is affected by the grain size and porosity of the sensor material. Future work would involve more extensive characterization of this relationship, coupled with developing a more complete understanding of the crystal lattice effects.
3. Identifying methods of enhancing the recovery of the sensor resistance after exposure to H<sub>2</sub>S. This gas has a tendency to remain on the sensor surface and must be removed to allow the resistance to return to its pre-exposure level. Pulsed heating methods, coupled with more extensive resistance testing to optimize operating temperature, would be applied.

All of these tasks are necessary for the continued development of these sensors. However, the multilayer architectures demonstrated during the Phase I project have established a solid basis from which this work can be performed during Phase II.

## 8. PUBLICATIONS

As of yet, no publications have resulted from this work. Should publications be prepared after submission of report, notification will be made to NIH.

## 9. REFERENCES

1. [www.biosystems.com/appnotes/perilsof.htm](http://www.biosystems.com/appnotes/perilsof.htm)
2. [www.instanet.com/~pfc/files/h2s.htm](http://www.instanet.com/~pfc/files/h2s.htm)
3. [cdalloz.com/9810.html](http://cdalloz.com/9810.html)
4. Hydrogen Sulfide in Workplace Atmospheres, OSHA method ID-141 ([www.osha-slc.gov/dts/slrc/methods/inorganic/id141/id141.html](http://www.osha-slc.gov/dts/slrc/methods/inorganic/id141/id141.html))
5. P. Szymanski, "H<sub>2</sub>S Monitoring/Datalogging in Manholes and Lift Stations," Industrial Hygiene News, [www.intlsensor.com/h2smonitoring.html](http://www.intlsensor.com/h2smonitoring.html)
6. Williams, D., *Sensors and Actuators B*, **57**, 1 (1999)
7. Ando, M. et al., *J. Mater. Chem.*, **4**, 631 (1994)
8. Yoo, D.J. et al., *J. Mater. Sci. Lett.*, **14**, 1391 (1995)
9. Ando, M. et al., *Chem. Lett.*, 335 (1994)
10. Vasiliev, R.B. et al., *Sensors and Actuators B*, **50**, 186, (1998)
11. Tamaki, J., *Sensors and Actuators B*, **49**, 121 (1998)
12. Mangamma, G., *Sensors and Actuators B*, **53**, 133 (1998)
13. Mistler, R.E., et al., "Tape Casting of Ceramics", pp. 414-448 in *Ceramic Processing Before Firing*, edited by G.Y. Onoda and L.L. Hench, New York: John Wiley and Sons, Inc., (1978).
14. J.S. Reed, *Introduction to Ceramic Processing*, NY: John Wiley and Sons, (1988).
15. R.E. Mistler, D.J. Shanefield, and R.B. Runk, "Tape Casting of Ceramics", pp. 414-448 in *Ceramic Processing Before Firing*, edited by G.Y. Onoda and L.L. Hench, New York: John Wiley and Sons, Inc., (1978).
16. J.S. Reed, *Introduction to the Principles of Ceramic Processing*, New York: John Wiley and Sons, Inc., (1988).
17. S.C. Moulzolf, et al., "Stoichiometry and Microstructure Effects on Tungsten Oxide Chemiresistive Films," *Sensors and Actuators B* **77** (2001) 375-82.
18. D. Fuller and A. Suruda, "Fatal Work-Related Deaths from Hydrogen Sulfide 1984-1994," [apha.confex.com/apha/128am/techprogram/paper\\_12231.htm](http://apha.confex.com/apha/128am/techprogram/paper_12231.htm)
19. M. Gayman, "Hydrogen Sulfide Kills," [www.swopnet.com/enr/Gayman/Gayman\\_H2S.html](http://www.swopnet.com/enr/Gayman/Gayman_H2S.html).
20. See OSHA - Standard Interpretations 04/25/1989 – Respiratory Protection Requirements for Sour Crude Oil Tank Operations", standard number 1910.134
21. "Preventing Deaths of Farm Workers in Manure Pits", NIOSH Alert, May 1990, publ # 90-103.
22. P. Szymanski, "H<sub>2</sub>S Monitoring/Datalogging in Manholes and Lift Stations," Industrial Hygiene News, [www.intlsensor.com/h2smonitoring.html](http://www.intlsensor.com/h2smonitoring.html)
23. [www.earthweshare.org/n/q\\_2001su\\_hogfactories.htm](http://www.earthweshare.org/n/q_2001su_hogfactories.htm)
24. [www.chron.com/content/chronicle/nation/h2s/chronology.html](http://www.chron.com/content/chronicle/nation/h2s/chronology.html)

Department of Health and Human Services  
**Final Invention Statement and Certification**  
(For Grant or Award)

DHHS Grant or Award No.  
1 R 43 OH07471-01

A. We hereby certify that, to the best of our knowledge and belief, all inventions are listed below which were conceived and/or first actually reduced to practice during the course of work under the above-referenced DHHS grant or award for the period.

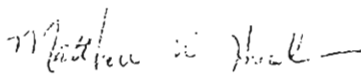
9/30/01 through 3/31/02  
*original effective date* *date of termination*

B. Inventions (Note: If no inventions have been made under the grant or award, insert the word "NONE" under Title below.)

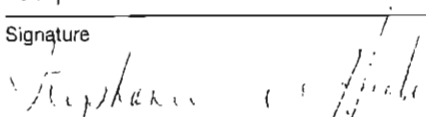
NAME OF INVENTOR	TITLE OF INVENTION	DATE REPORTED TO DHHS
	None	

(Use continuation sheet if necessary)

C. **First Signature** — The person responsible for the grant or award is required to sign (in ink). Sign in the block opposite the applicable type of grant or award.

TYPE OF GRANT OR AWARD	WHO MUST SIGN (title)	SIGNATURE
Research Grant SBIR Phase I	Principal Investigator or Project Director Matthew Hooker, PI	
Health Services Grant	Director	
Research Career Program Award	Awardee	
All other types (specify):	Responsible Official	

D. **Second Signature** — This block **must** be signed by an official authorized to sign on behalf of the institution.

Title Business Development Manager	Name and Mailing Address of Institution Nanomaterials Research LLC 2021 Miller Drive Suite B Longmont, CO 80501
Typed Name Stephanie Hooker	
Signature 	



## Equipment Inventory

NIH Contract 1 R43 OH07471-01  
SBIR Phase I

Nanomaterials Research LLC  
2021 Miller Drive  
Suite B  
Longmont, CO 80501

Tel: (720) 494-8401  
Fax: (720) 494-8402

No equipment was purchased during this project.